INDO-US WORKSHOP ON NANOSONICS & ULTRASONICS AND INTERNATIONAL CONFERENCE ON NANOTECHNOLOGY AND ULTRASOUND

I
U
W
O
N
U
&
I
C
N
U
2011

12-14 January 2011

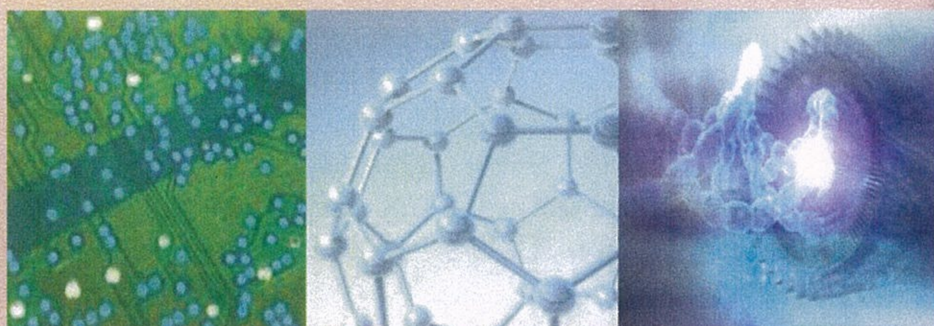

Proceedings

Organized by

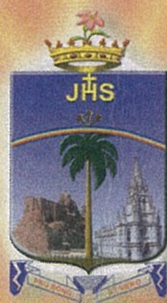

DEPARTMENT OF PHYSICS
St. JOSEPH'S COLLEGE (Autonomous)
Reaccredited with A+ Grade
College with Potential for Excellence
TIRUCHIRAPPALLI - 620 002, INDIA

TEM Studies of SPUTTER-DEPOSITED Ni_4Al Alloy Thin Films

T. Joseph .Sahaya Anand

Department of Engineering Materials, Faculty of Manufacturing Engineering, University Technical Malaysia Melaka (UTeM), 76109 Durian Tunggal, Melaka, MALAYSIA.

Abstract: The nanostructural characteristics of direct-current magnetron sputter-deposited Ni_4Al alloy films were studied during in situ isothermal annealing in a transmission electron microscope. An expansion of the lattice by nearly 5% was observed for the $Ni_{0.8}Al_{0.2}$ films in their low-thickness and as-deposited state. The lattice size approaches the bulk value when the film thickness increases or after vacuum annealing heat-treatment. The $Ni_{0.8}Al_{0.2}$ films have a nanocrystalline structure in which the ordered $L1_2$ phase appears upon annealing at above 500°C. The ordered B2 phase Ni_4Al phase with orthorhombic structure were found.

Keywords: dc magnetron sputtering, crystallographic structure, transmission electron microscope, thin film

INTRODUCTION

Nickel aluminides have attracted a lot of attention in the past as structural materials for high-temperature applications. More recently, they are being studied for potential use as functional coatings for engineering applications ranging from aero engines to microelectronic devices [1-3]. A number of micro structural studies have been carried out on nickel aluminide coatings in the last few years [4-8]. For example, Almeida *et al.* [4] and the present authors [5-6] have studied the microstructures of Ni_3Al thin films in relation to their lattice parameter misfits. Schryvers *et al.* studied the *in situ* TEM study of the Ni_5Al_3 properties useful in magnetic studies [7]. Liu *et al.* used the laser interference pattern to activate the intermetallic reaction between Ni and Al atoms in the stoichiometric ratio 3:1 to solve the problems of plasticity and brittleness for the intermetallic compounds [9]. Banerjee studied the hardness of sputter deposited nanocrystalline Ni_3Al thin films [10].

In our previous reports, we demonstrated that direct-current (dc) magnetron sputter-deposited $Ni_{0.8}Al_{0.2}$ thin films exhibit a phenomenal electrical transition from an insulating state to a conduction state upon mild heating only when x = 0.75 and 0.8 [11]. The transition effect is found to be reversible with respect to temperature changes, implying that the transition happens at constant microstructure. This is to be distinguished from another effect of electrical resistance variation due to annealing of the film's microstructures. The as-deposited state of the $Ni_{0.75}Al_{0.25}$ films is known to be nanocrystalline with a typical grain size of the order of few nanometres [4, 8]. The reversible transition is found to occur over a temperature range from room temperature to about 250°C, within which grain growth is suppressed. One possible application of the reversible transition effect in nanocrystalline $Ni_{0.75}Al_{0.25}$ and $Ni_{0.8}Al_{0.2}$ thin films would be as thermal switches in microelectromechanical systems, but the applicability hinges on the thermal stability of the film with respect to grain growth and other micro structural changes.

There are at least two reasons why grain growth in nanocrystalline materials can be potentially very different from the situation in conventional large grained materials. The first is the absence of dislocations in the nanocrystalline state, and hence one would not expect recovery or recrystallization to precede grain growth. This point is of crucial importance to processing routes involving ball milling in the powder metallurgy [12]. Secondly, the

**Corresponding author: Tel. + 6(06)3316489; Fax. + 6(06)3316411*
E-mail. anand@utem.edu.my (T. Joseph Sahaya Anand)

physical dimension of the grain boundaries in a nanocrystalline material would limit the formation of conventional second phase particles in large grained materials, and hence the conventional Zener drag mechanism of grain boundary pinning would no longer be applicable. Hence the present paper represents the micro structural study of nanocrystalline $Ni_{0.8}Al_{0.2}$ thin films to find out the correlation between the microstructure and electrical transition.

MATERIALS AND METHODS

The $Ni_{0.8}Al_{0.2}$ thin films were synthesized by a water-cooled, low-power dc magnetron sputtering device (BAL-TEC MED 020) using the corresponding nickel aluminium alloy target. The sputtering chamber was evacuated with the base pressure maintained at about 4.0×10^{-6} mbar, and a continuous flux of ultra high purity (> 99.9999 %) argon was introduced at a pressure of 5×10^{-2} mbar during film deposition. Pre-sputtering of the target was performed at least three times with duration of 15 minutes each time, followed by flushing with high-purity argon to remove excessive oxygen and other residual gases. Carbon films supported by 3mm-diameter copper grids to produce plan-view samples were used as substrates for micro structural analyses by *in-situ* transmission electron microscopy (TEM). These films were deposited at a sputtering power of 30 W and the alloy target was placed 60mm above the substrate stage. Although there was no additional thermal source applied to the substrates during the deposition process, the substrates became warmed up to nearly 60°C by the plasma-discharge heating. The deposition rate was measured to be approximately 2 – 3 Å/sec and the film thickness was controlled by means of deposition time.

Micro structural examination was carried out in a JEOL 2000-FX TEM operating at 200 kV as well as a Philips Tecnai TEM. It is very essential that the sample be thin enough for the electrons to penetrate. For instance, it should not be thicker than 200nm, for a TEM having an electron gun of 200kV. The crystal structures of the films were analysed by selected area diffraction (SAD). *In situ* annealing inside the TEM was carried out on as-deposited films to study the micro structural changes during heating. Post-deposition heat treatment of the films was carried out with a Carbolite vacuum furnace at a vacuum of about 1×10^{-6} mbar for 2 hours followed by furnace cool to enhance their crystallinity in the TEM for comparison purposes. JEOL 2010F TEM operating at 200 kV with field emission gun was also used for HRTEM analysis mainly for low thickness films. This microscope has the lattice resolution of 0.102 nm which has been used to obtain the information of the nanograin compositions.

RESULTS

To study the structural properties of $Ni_{0.8}Al_{0.2}$thin films, TEM was chosen to examine their nano-crystalline structure and internal build-up of the films to a finer extent. To study the grain growth kinetics as a function of time and temperature, dynamic micro structural observations were carried out on the TEM specimens during a series of isothermal *in situ* heat treatments. Figs. 1- 2 show the bright field images during *in situ* annealing as well as post-deposition annealing of the $Ni_{0.8}Al_{0.2}$thin films and the corresponding SAD patterns with structural calculations as far as possible. In these experiments, the films were heated *in situ* from room temperature to 700°C. A constant heating rate of 8 – 10 °C/min was used for all temperature increments throughout the heating.

Post deposition annealing was carried out at a vacuum of 2.0 x 10^{-6} mbar for 2 hours. Crystallographic information of the films was obtained by selected area diffraction (SAD) pattern. An SAD aperture about 120 nm in size was used to select the region for diffraction, and a needle head was positioned to block the transmitted beam to allow better exposure of the weaker diffracted beams. The lattice constant is deduced from the observable diffraction rings according to the relationship

$$g = \frac{\sqrt{h^2 + k^2 + l^2}}{a} = \frac{X_{hkl}}{L\lambda} \qquad (1)$$

in the case of cubic structure, and for films having an orthorhombic structure, the lattice constant is deduced from the relationship

$$g = \sqrt{\frac{h^2}{a^2} + \frac{k^2}{b^2} + \frac{l^2}{c^2}} = \frac{X_{hkl}}{L\lambda} \qquad (2)$$

where a, b and c are the lattice parameters, (hkl) is the diffraction plane indices, X_{hkl} the radius of the diffraction ring, λ the electron wavelength and L the camera length. For a series of diffraction rings, $\sqrt{h^2 + k^2 + l^2}$ should then be proportional to X_{hkl}, the proportionality constant being a/Lλ for cubic structure.

And for the orthorhombic structure $\sqrt{\frac{h^2}{a^2}+\frac{k^2}{b^2}+\frac{l^2}{c^2}}$ is proportional to X_{hkl}. Here the values of X_{hkl} were measured by software called Process Diffraction [13] from SAD patterns digitized at a resolution of 300 dpi, which offers an equivalent instrumental resolution of better than 85 μm on a photographic print. Based on the above equations, the lattice constants for the films during both *in situ* annealing as well as post-deposition annealing were calculated, and the results with the corresponding crystallographic structures also presented. Because the intensities of higher-order diffraction rings attenuate rather quickly, the analyses were restricted to the first few rings.

Fig. 1 shows the *in situ* annealing results of $Ni_{0.8}Al_{0.2}$ thin films with thickness of about 130 nm. The SAD

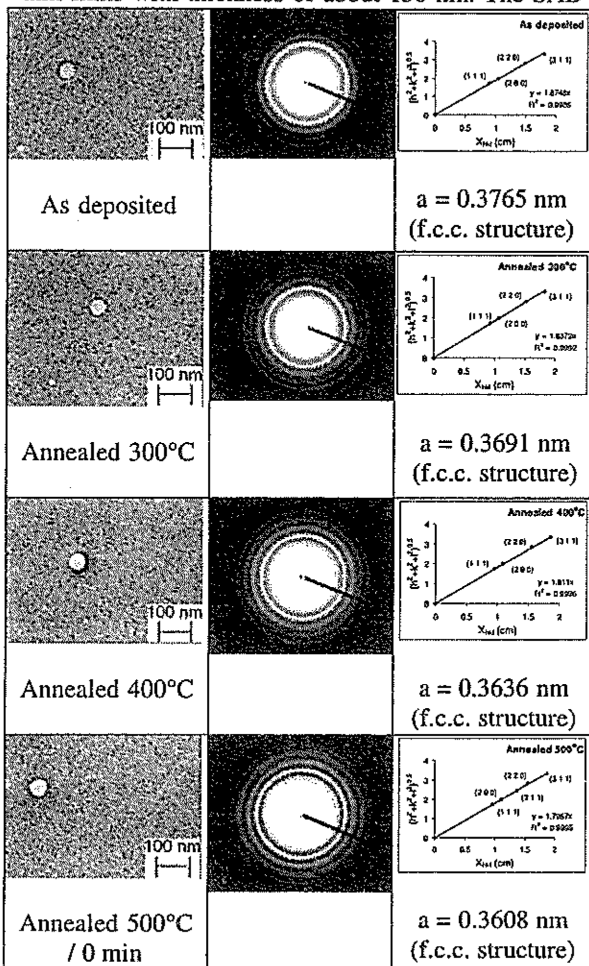

pattern of the corresponding isothermal heating shows the occurrence of a disordered f.c.c. structure in the as-deposited state. The SAD pattern of the as-deposited film in fig. 1 shows only the fundamental f.c.c. reflections (111), (200), (220) and

Fig. 1 *in situ* TEM analysis of $Ni_{0.8}Al_{0.2}$ thin films showing the grain growth 500°C

(311), and the same structure persists until the temperature attains 500°C.

Although the film has the stoichiometric $Ni_{0.8}Al_{0.2}$ composition, it is still not surprising from the previous XRD results that the ordered $L1_2$ super lattice structure would not be established at low temperatures [11]. However the lattice parameter as deduced from the slope of the linear fit of the as-deposited film is 0.3765 nm, which is about 5.4 % greater than the bulk value of ordered Ni_3Al. at

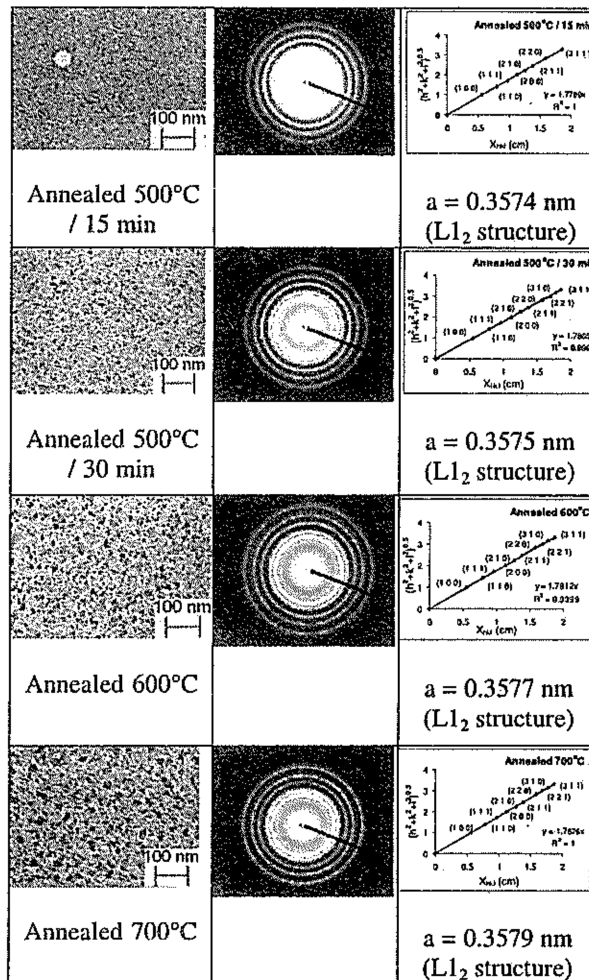

Fig. 1 *in situ* TEM analysis of $Ni_{0.8}Al_{0.2}$ thin films showing the grain growth 500°C (Contd.)

500°C, a relatively weak ring appeared in between the (200) and (220) reflections and this can be indexed as the {211} super lattice reflection corresponding to the

ordered $L1_2$ phase. It shows that the ordering of the Ni-Al lattice might have

initiated at this temperature. Besides the {211} reflection, the lower order {100} and {110} super lattice reflections also appeared after increasing the annealing time at 500°C, as shown in fig. 1.

Similar results were also obtained from the post-deposition annealed TEM results shown in fig. 2. The grain size also increases to a few hundreds of nm under the elevated annealing temperature, from the few nanometres in the as-deposited state. Table 1 summarizes the lattice enlargement observed during the *in situ* annealing experiment shown in fig. 1.

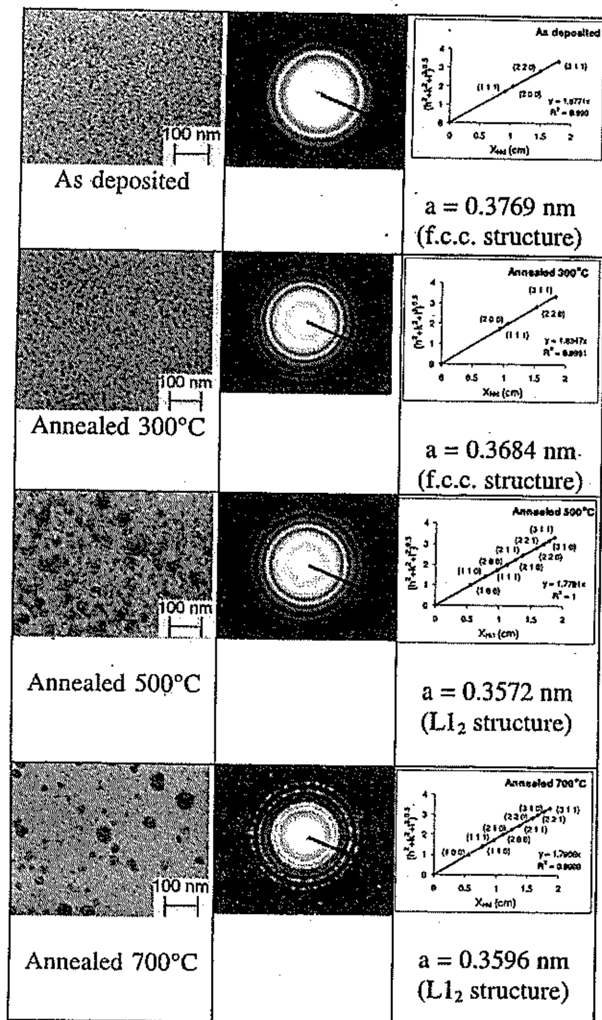

Fig.2 TEM analysis of post deposition annealed $Ni_{0.8}Al_{0.2}$ thin films showing the lattice constant expansion

HRTEM was also performed on selected samples. Fig 3 shows some HRTEM images of $Ni_{0.8}Al_{0.2}$ thin films with thickness about 110 nm. The grain size distribution is evidently uniform in the as-deposited state, as shown in fig. 3(a). After annealing at 700°C, some grains grow abnormally to as large as 120 nm as shown in fig. 3(b), from the initial a few nanometres in the as-deposited state. The HRTEM image in fig. 3(c) shows that the abnormally grown grains have a fringe width of 0.2 nm in the d spacing of about 0.2074 nm which corresponds to $Ni_{0.8}Al_{0.2}$ (1 1 1) plane.

Table 1. Lattice parameter enlargement of $Ni_{0.8}Al_{0.2}$ thin films as observed from *in situ* TEM annealing. Lattice constant of bulk Ni_3Al = 0.3572 nm. Camera length L = 80 cm and λ = 0.0025 nm for 200 keV.

$Ni_{0.8}Al_{0.2}$ film	Slope	Lattice constant a (nm)	% Lattice enlargement
As deposited	1.8748	0.3765	5.40
Annealed 300°C	1.8379	0.3691	3.33
Annealed 400°C	1.8110	0.3636	1.79
Annealed 500°C / 0 min	1.7967	0.3608	1.01
Annealed 500°C / 15 min	1.7799	0.3574	0.06
Annealed 500°C / 30 min	1.7805	0.3575	0.08
Annealed 600°C	1.7812	0.3577	0.14
Annealed 700°C	1.7826	0.3579	0.20

During high-temperature annealing grain coalescence was observed, and fig. 3(d) shows the junction between two coalescing grains, which themselves have grown abnormally out from the nanocrystalline matrix. The abnormally grown grains are sometimes faulted; examples of this are shown in figs. 3(e) and (f). The faults seen in these two figures may be nano-twins.

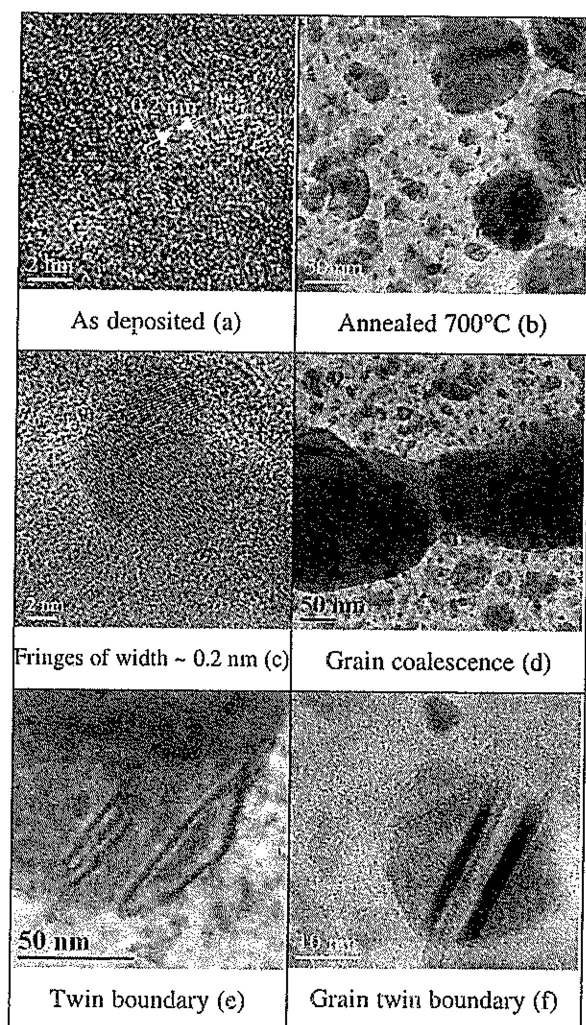

Fig. 3 High resolution TEM analysis of $Ni_{0.8}Al_{0.2}$ showing the fringes and twin boundaries in the annealed conditions of 110 nm thick film (a) As deposited film (b) – (f) 700°C annealed $Ni_{0.8}Al_{0.2}$ film.

Fig. 4 shows a sequence of abnormal grain growth and grain coalescence processes recorded from a $Ni_{0.8}Al_{0.2}$ film *in situ* annealed at 500°C for different times. The series of images were taken at 15 minutes' time interval. A tendency can be observed from the figures for the nanograins to coalesce to form larger grains of a few tens of nanometres. Grain coalescence was indeed observed to be the main mechanism responsible for the accelerated grain growth at high temperatures. After two grains have grown to make an initial contact, the subsequent merging process seems to be movements of the two grains towards each other, possibly by a viscous flow process.

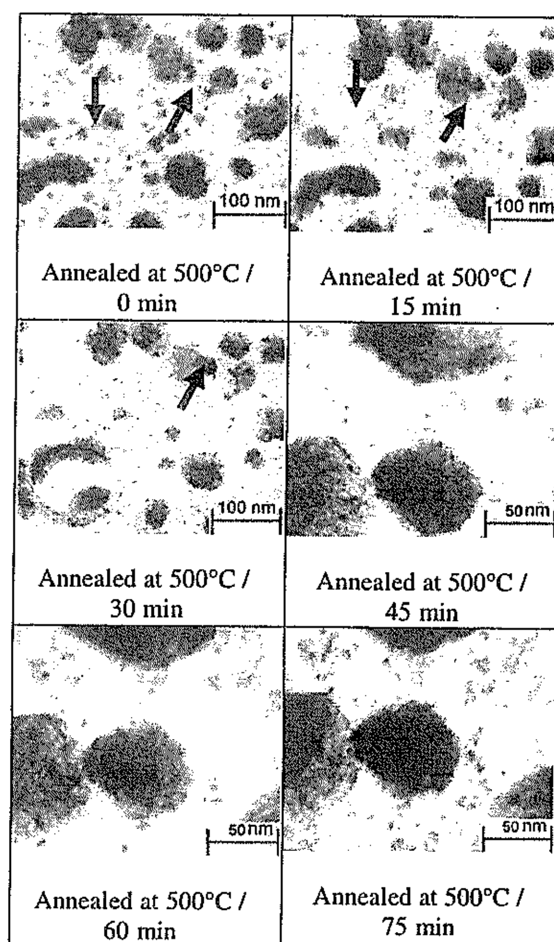

Fig. 4 TEM analysis of $Ni_{0.8}Al_{0.2}$ showing the grain coalescence after *in situ* annealing 500°C.

DISCUSSION

Planar TEM investigations were carried out to examine the relationship between the electrical transition and the microstructures of the $Ni_{0.8}Al_{0.2}$ films. TEM/SAD micrographs also indicated a trend of nano-structural and crystallographic changes upon annealing the $Ni_{0.8}Al_{0.2}$ film. Although the films remain nano-crystalline in nature, some crystals exhibit growth as the deposition temperature increased. The SAD pattern of the corresponding

isothermal heating of nanocrystalline $Ni_{0.8}Al_{0.2}$ thin film shows the occurrence of a disordered f.c.c. structure in the as-deposited state. Although the film has the stoichiometric $Ni_{0.8}Al_{0.2}$ composition, it is yet not surprising from the previous results that the ordered $L1_2$ super lattice structure would not be established at low temperatures. The contrast of the grains is the diffraction contrast caused by the difference in orientation of the grains suggesting that the samples are polycrystalline in nature. Plane-view TEM bright field images show that grain size increases with increasing the temperature of the film. The temperatures at which the $Ni_{0.8}Al_{0.2}$ phase was observed to form was found in the temperature range of 300 - 350°C. During high temperature annealing (above 500°C) grain coalescence was observed (fig. 4) and this can be the main reason for the abnormal grain growth in these temperatures.

CONCLUSIONS

The normal grain growth kinetics under *in situ* isothermal heating in TEM was analyzed and abnormal grain growth observed in the high annealed films. The $Ni_{0.8}Al_{0.2}$ films have a nanocrystalline structure in which the ordered $L1_2$ phase with a lattice constant of 0.357 nm appears during post-deposition annealing at above 500°C. A significant lattice expansion is observed in the $Ni_{0.8}Al_{0.2}$ films in the as-deposited state with 5.4 % expansion. However, annealing the samples around 500°C make the lattice size approach the corresponding bulk value. There is a general trending of grain coalescence to happen in the $Ni_{0.8}Al_{0.2}$ thin films during *in situ* annealing above 500°C.

ACKNOWLEDGEMENT

The work described in this paper was supported by Universiti Teknikal Malaysia Melaka (UTeM) short term grant (Project No. PJP/2009/FKP (23A) S628).

REFERENCES

[1] Lee, H.Y., Ikenaga, A., Kim, S.H. and Kim, K.B. (2007) The effects of induction heating rate on properties of NiAl based intermetallic compound layer coated on ductile cast iron by combustion synthesis *Intermet.* 15: 1050-1056.

[2] Sierra, C. and Va´zquez, A.J. (2006) NiAl coating on carbon steel with an intermediate Ni gradient layer", *Surf. Coat. Technol.* 200: 4383-4388.

[3] Li, P.Y., Lu, H.M., Tang, S.C. and Meng, X.K., (2009) An in-situ TEM investigation on microstructure evolution of Ni-25 at.% Al thin films, *Journal of Alloys and Compounds* 478 (1-2): 240-245.

[4] de Almeida, P., Schäublin, R., Almazouzi, A., Victoria M. and Lévy, F. (2000) Microstructure and growth modes of stoichiometric NiAl and Ni_3Al thin films deposited by r.f. –magnetron sputtering, *Thin Solid Films.* 368: 26-34.

[5] Meng, X.K. and Ngan, A.H.W. (2004) Nano-alloys synthesized by controlled crystallization from super cooled atomic clusters of elements *J. Mater. Res.* 19: 780-785.

[6] Ng, H.P. and Ngan, A.H.W. (2002) An in situ transmission electron microscope investigation into grain growth and ordering of sputter-deposited nanocrystalline Ni_3Al thin films, *J. Mater. Res.* 17: 2085-2094.

[7] Schryvers, D. and Ma, Y. (1995) In-Situ TEM study of the Ni_5Al_3 to $B2+Ll_2$ decomposition in $Ni_{65}Al_{35}$ *Mater. Lett.* 23: 105-111.

[8] Ng, H.P. and Ngan, A.H.W. (2000) Metal-to-insulator transition in sputter deposited 3Ni/Al thin films. *J. Appl. Phys.* 88 (5): 2609-2616.

[9] Liu, Z., Xuede, Y., Ping, Z., Guang, H., Xuehui, L. Recktenwald T. and Mücklich, F. (2007) Spatially resolved intermetallic reaction of Ni_3Al by laser interference structuring, *Intermet* 15: 796-800.

[10] Banerjee, R. (2007) Hardness of sputter deposited nanocrystalline Ni_3Al thin films. *Mater. Lett.* 61: 609-612.

[11] Anand, T.J.S., Ng, H.P. Ngan, A.H.W. and Meng, X.K. (2003) Temperature-coefficient-of-resistance characteristics of sputter-deposited Ni_xAl_{1-x} thin films for 0.5< x < 1", *Thin solid films*, 441: 298-306.

[12] Tellkamp, V.L. Dallek, S. Cheng, D. and Lavernia, E.J. (2001) Grain growth behavior of a nanostructured 5083 Al-Mg alloy, *J. Mater. Res.* 16: 938-944.

[13] Lábár, J.L. (2000) Process Diffraction: A computer program to process electron diffraction patterns from polycrystalline or amorphous samples". Proc. of EUREM 12, Brno I 379 – I 380.